iScience, Volume *27*

Supplemental information

Transient titin-dependent ventricular defects during development lead to adult atrial arrhythmia and impaired contractility

Xinghang Jiang, Olivia T. Ly, Hanna Chen, Ziwei Zhang, Beatriz A. Ibarra, Mahmud A. Pavel, Grace E. Brown, Arvind Sridhar, David Tofovic, Abigail Swick, Richard Marszalek, Carlos G. Vanoye, Fritz Navales, Alfred L. George Jr., Salman R. Khetani, Jalees Rehman, Yu Gao, Dawood Darbar, and Ankur Saxena

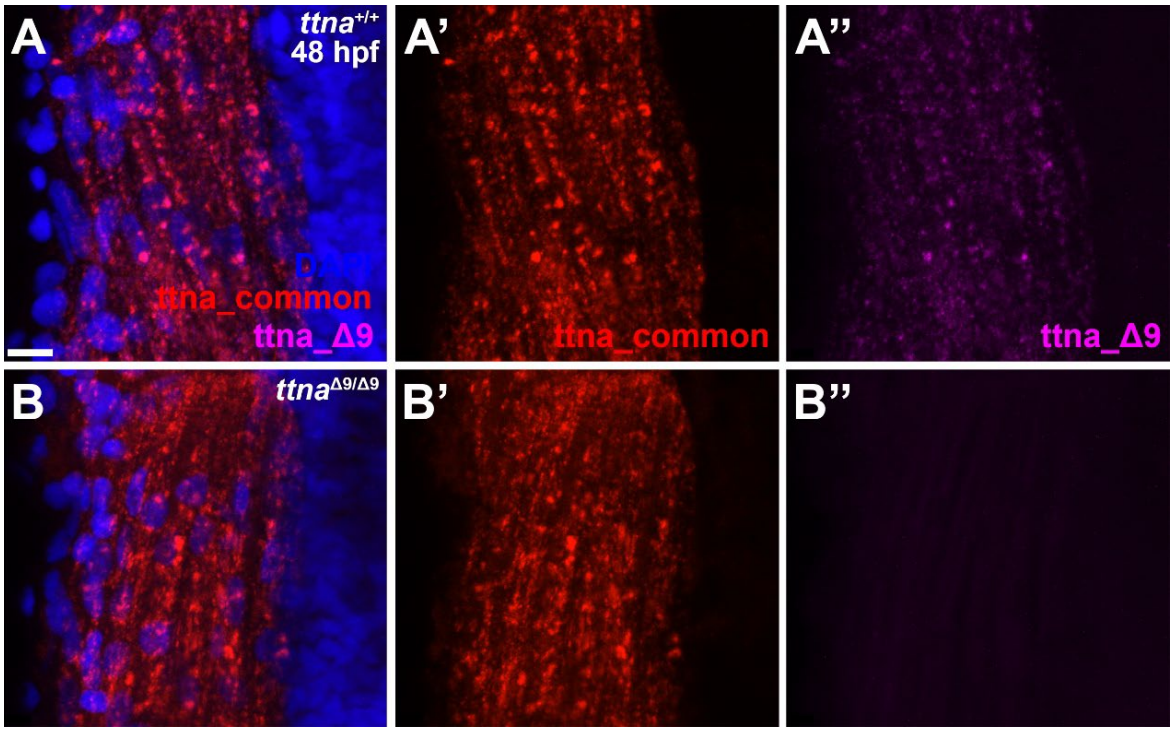

Figure S1. *ttna*$^{\Delta 9}$ deletion detected in skeleton muscle, related to Figure 1.
Representative images of *in situ* hybridization chain reaction with probes targeting *ttna* mRNA in either the 27 base pair-deleted region (ttna_Δ9, magenta) or regions approximately 1500 base pairs upstream and downstream of the deletion (ttna_common, red) in skeletal muscle of wild-type (*ttna*$^{+/+}$, n = 6, **A-A''**) and *ttna*$^{\Delta 9/\Delta 9}$ (n = 6, **B-B''**) zebrafish embryos at 48 hours post-fertilization (hpf). Scale bar: 10 μm.

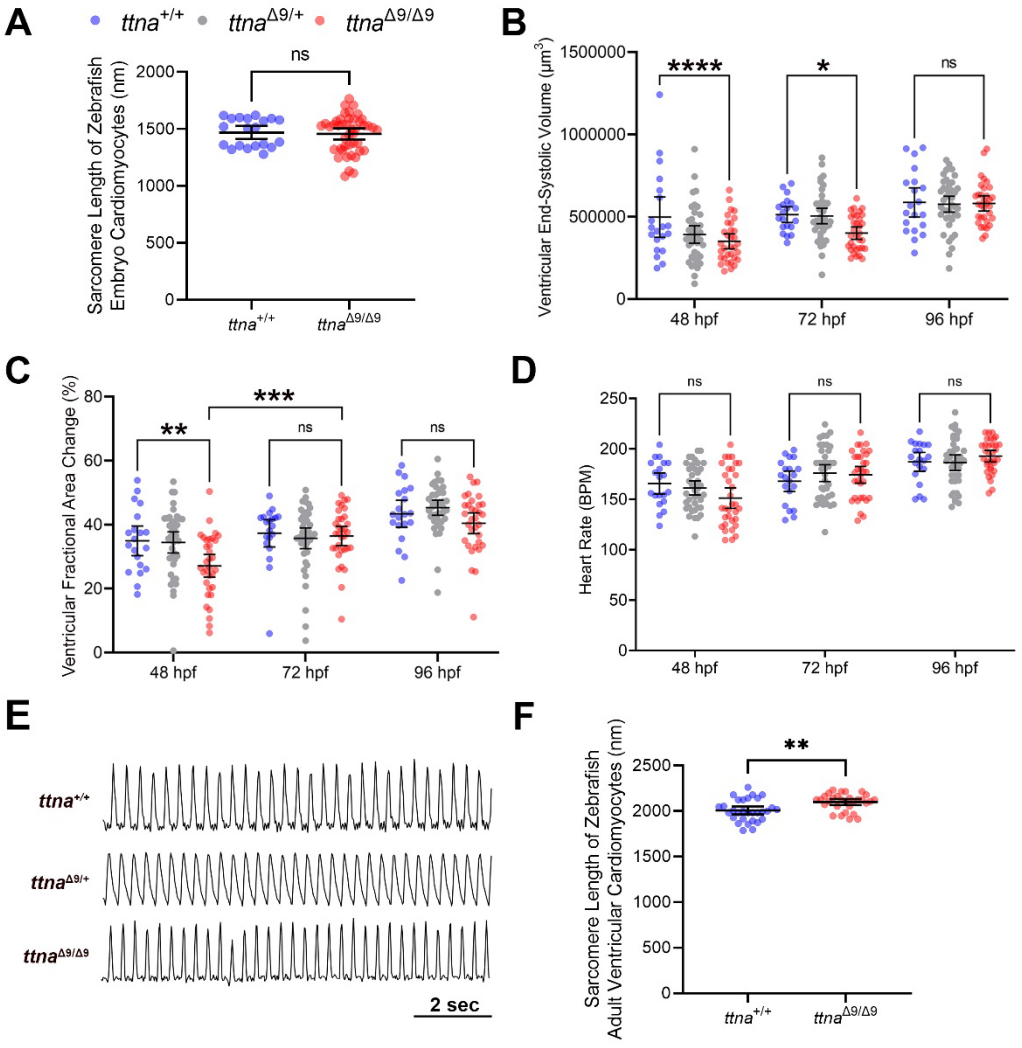

Figure S2. *ttna*$^{\Delta 9/\Delta 9}$ zebrafish embryos exhibit normal sarcomere length, heart rate, and rhythm and reduced ventricular size and contraction that recover rapidly, related to Figure 2.

(**A**) Length of sarcomeres in *ttna*$^{+/+}$ and *ttna*$^{\Delta 9/\Delta 9}$ embryo cardiomyocytes at 48 hpf. Seven to ten sarcomere lengths from each embryo (embryo number: *ttna*$^{+/+}$ = 2, *ttna*$^{\Delta 9/\Delta 9}$ = 5) were combined for each genotype. (**B-D**) Quantification of ventricular end-systolic volume (**B**), fractional area change (**C**), and heart rate (**D**) for *ttna*$^{+/+}$, *ttna*$^{\Delta 9/+}$, and *ttna*$^{\Delta 9/\Delta 9}$ embryos at 48, 72, and 96 hpf. (**E**) Representative beating pattern of *ttna*$^{+/+}$, *ttna*$^{\Delta 9/+}$, and *ttna*$^{\Delta 9/\Delta 9}$ embryos at 48 hpf. (**F**) Length of sarcomeres in *ttna*$^{+/+}$ and *ttna*$^{\Delta 9/\Delta 9}$ adult ventricular cardiomyocytes at 6 months age. Ten sarcomere lengths from each zebrafish (zebrafish number: *ttna*$^{+/+}$ = 3, *ttna*$^{\Delta 9/\Delta 9}$ = 3) were combined for each genotype. n value for (**B-E**): *ttna*$^{+/+}$ = 20, *ttna*$^{\Delta 9/+}$ = 39, *ttna*$^{\Delta 9/\Delta 9}$ = 33. Data in (**A-D, F**) are represented as mean ± 95% confidence intervals. ns $p > 0.05$; * $p < 0.05$; ** $p < 0.01$; *** $p < 0.001$; **** $p < 0.0001$.

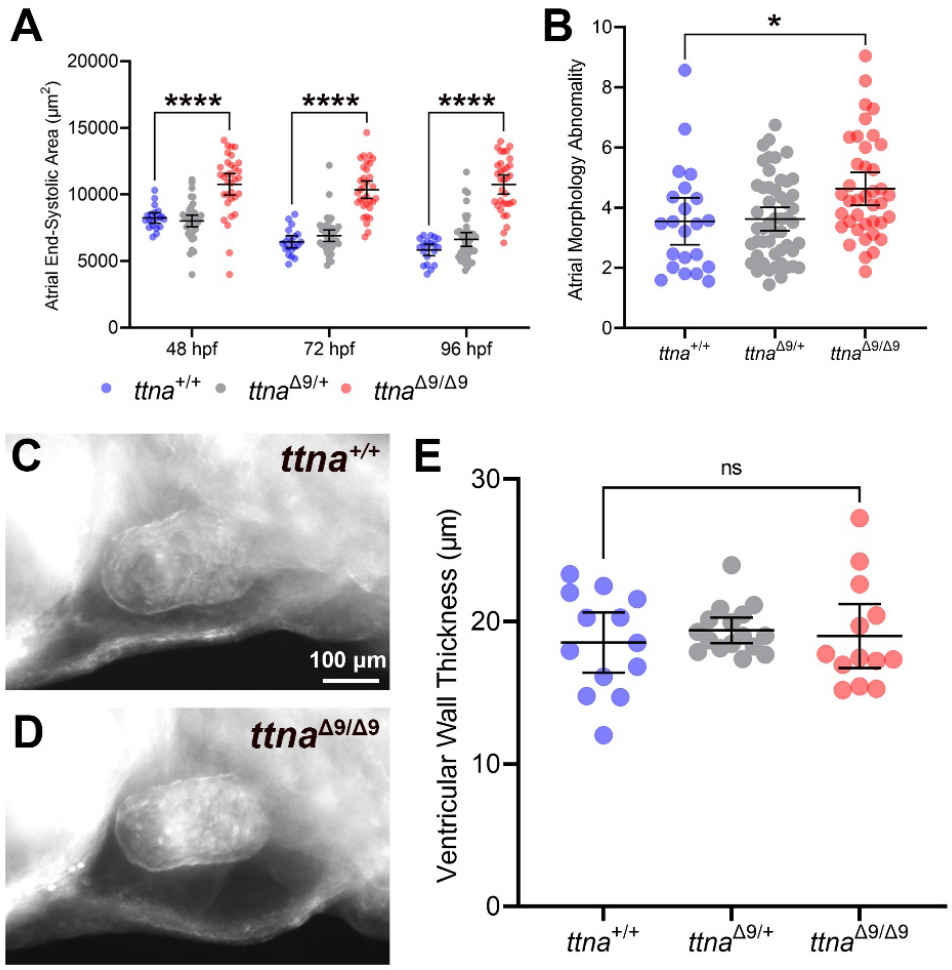

Figure S3. *ttna*$^{\Delta 9/\Delta 9}$ zebrafish embryos' atria exhibit enlargement and abnormal shape while ventricles show normal morphology and wall thickness, related to Figure 3.
(**A**) Quantification of atrial end-systolic area for *ttna*$^{+/+}$ (n = 20), *ttna*$^{\Delta 9/+}$ (n = 39), and *ttna*$^{\Delta 9/\Delta 9}$ (n = 33) zebrafish embryos at 48, 72, and 96 hpf. (**B**) Quantification of atrial shape abnormality at 96 hpf. n value: *ttna*$^{+/+}$ = 22, *ttna*$^{\Delta 9/+}$ = 49, *ttna*$^{\Delta 9/\Delta 9}$ = 41. (**C-E**) Representative images of 96 hpf *ttna*$^{+/+}$ and *ttna*$^{\Delta 9/\Delta 9}$ zebrafish ventricles and blood visualized with brightfield and the red blood cell-labeling transgenic line gata1:dsRed, respectively. (**E**) Quantification of the ventricular myocardial wall thickness of *ttna*$^{+/+}$, *ttna*$^{\Delta 9/+}$, and *ttna*$^{\Delta 9/\Delta 9}$ zebrafish embryos at 96 hpf. Data in (**A-B, E**) are represented as mean ± 95% confidence intervals. n value (**C-E**): *ttna*$^{+/+}$ = 13, *ttna*$^{\Delta 9/+}$ = 16, *ttna*$^{\Delta 9/\Delta 9}$ = 13. ns $p > 0.05$; * $p < 0.05$; **** $p < 0.0001$.

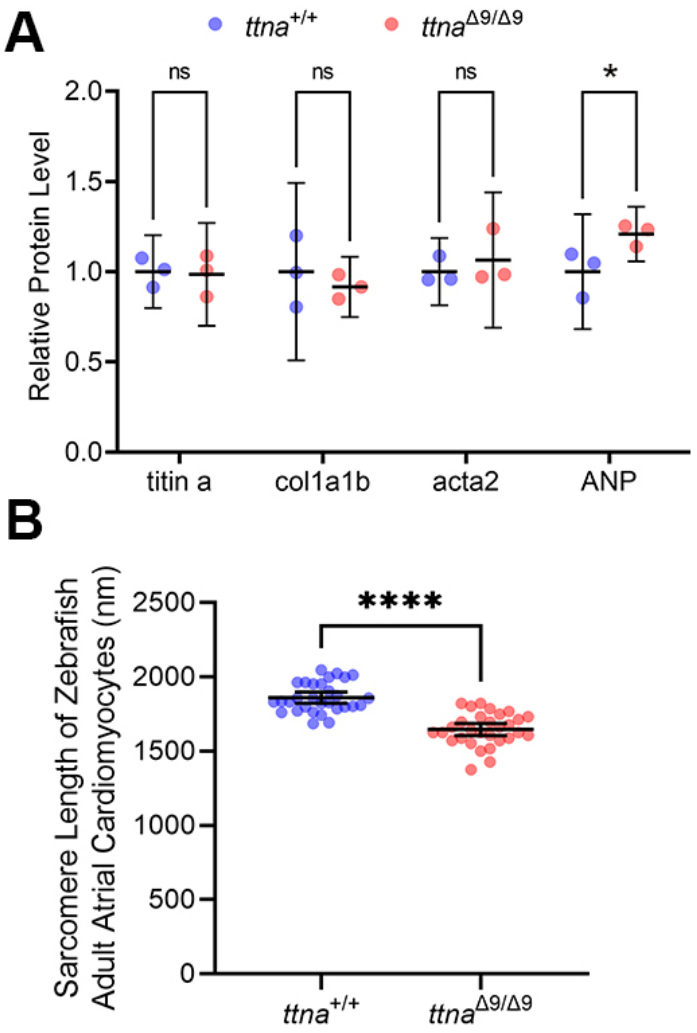

Figure S4. *ttna*$^{\Delta 9/\Delta 9}$ adult zebrafish atria exhibit unchanged levels of titin and fibrosis-related proteins, shortened sarcomere length, and elevated ANP and BNP levels, related to Figures 2-4.

(**A**) Quantification of the relative expression levels of titin a, col1a1b, acta2, ANP, and BNP from *ttna*$^{+/+}$ and *ttna*$^{\Delta 9/\Delta 9}$ zebrafish atrial proteomics at 7 months age. Each data point consists of a sample pooled from 10 atria. (**B**) Length of sarcomeres in *ttna*$^{+/+}$ and *ttna*$^{\Delta 9/\Delta 9}$ adult atrial cardiomyocytes at 6 months age. Ten sarcomere lengths from each zebrafish (zebrafish number: *ttna*$^{+/+}$ = 3, *ttna*$^{\Delta 9/\Delta 9}$ = 3) were combined for each genotype. Data are represented as mean ± 95% confidence intervals. ns $p > 0.05$; * $p < 0.05$; **** $p < 0.0001$.

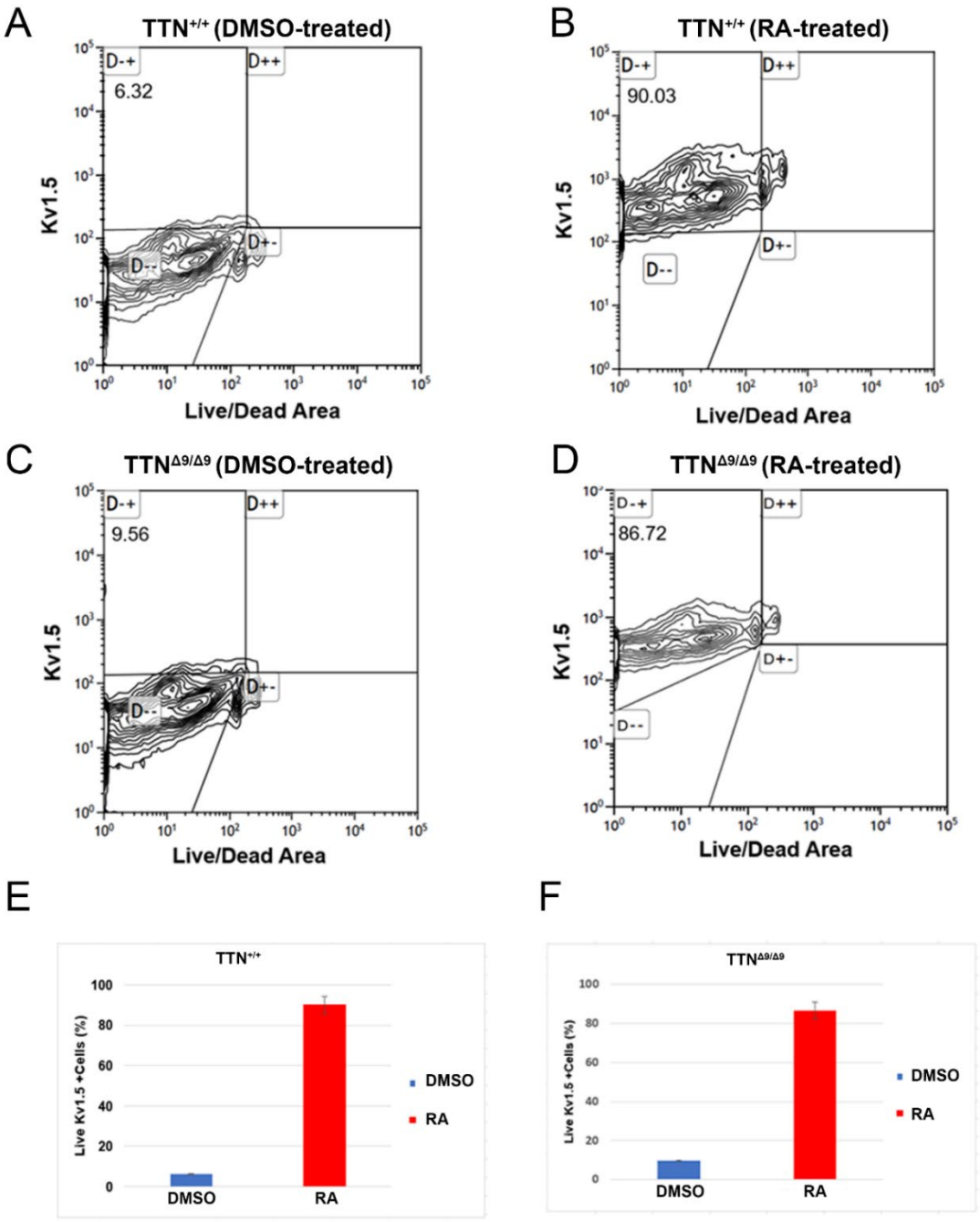

Figure S5. Retinoic acid was used to induce hiPSC-aCM differentiation from hiPSCs, related to Figure 3.

(**A-B**) Representative flow cytometry contour plots of retinoic acid (RA)-treated and dimethyl sulfoxide (DMSO)-treated *TTN*$^{+/+}$-hiPSC-aCMs sorted into Kv1.5 positive and live fractions at day 10 (quadrant 1, upper left). (**C-D**) Representative flow cytometry contour plots of RA-treated and DMSO-treated *TTN*$^{\Delta 9/\Delta 9}$-hiPSC-aCMs sorted into Kv1.5 positive and live fractions at day 10 (quadrant 1, upper left). (**E-F**) Averaged flow cytometry data from *TTN*$^{+/+}$-hiPSC-aCMs and *TTN*$^{\Delta 9/\Delta 9}$-hiPSC-aCMs. Data in (**E-F**) are represented as mean ± 95% confidence intervals.

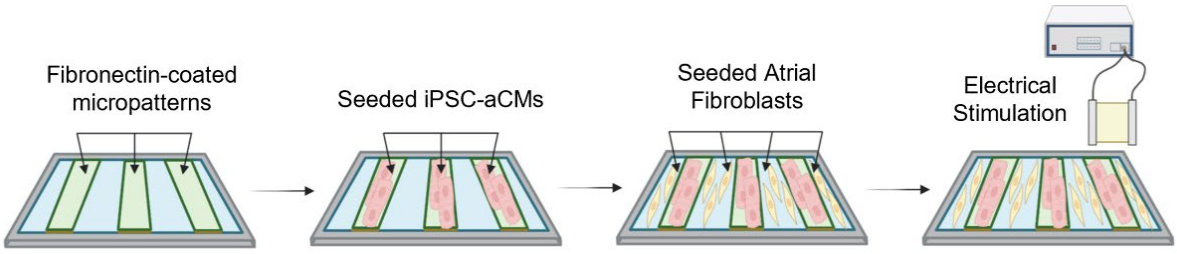

Figure S6. Development and fabrication of hiPSC-aCM modeling platform, related to Figure 3.

A micropatterned co-culture approach, with the addition of electrical stimulation, was used in order to mature hiPSC-aCMs post-differentiation. Fibronectin micropatterns with a width of 55 μm and a spacing of 80 μm were created on tissue culture plates. HiPSC-aCMs were seeded and preferentially attached to the micropatterns, and cardiac fibroblasts isolated from human atrial tissue were subsequently seeded to fill in the spaces between hiPSC-aCM micropatterns. Electrical stimulation was applied on the micropatterned cocultures.

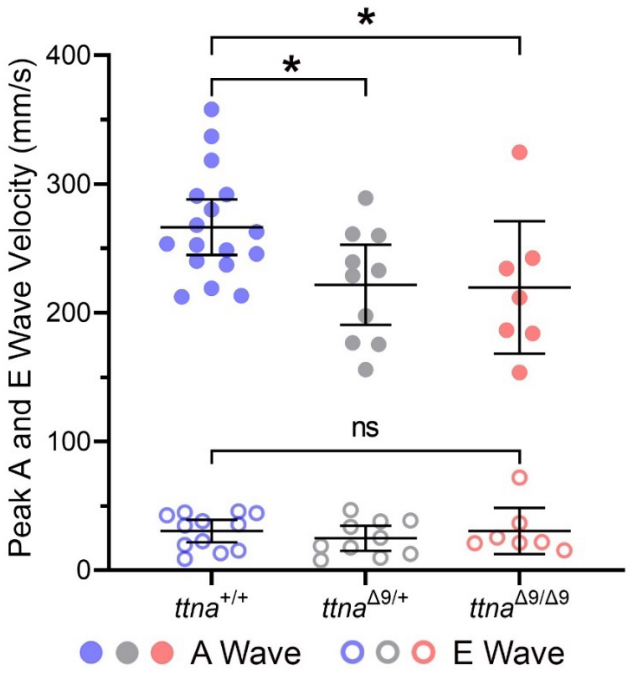

Figure S7. *ttna*$^{\Delta 9/\Delta 9}$ adult zebrafish atria have reduced contraction, related to Figure 4. Quantification of peak A and E wave velocities from echocardiography of 14-15 months old *ttna*$^{+/+}$, *ttna*$^{\Delta 9/+}$, and *ttna*$^{\Delta 9/\Delta 9}$ zebrafish. Data are represented as mean ± 95% confidence intervals. ns $p > 0.05$; * $p < 0.05$.

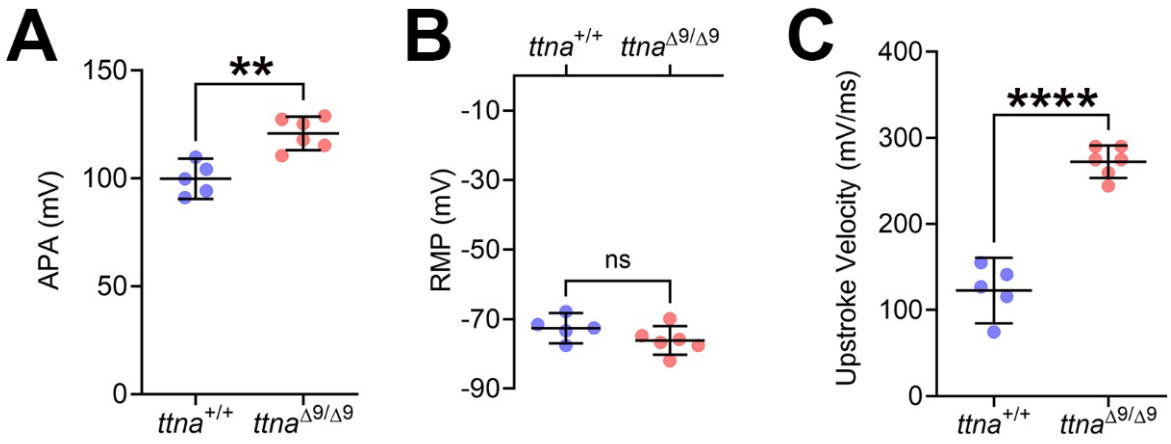

Figure S8. *ttna*$^{\Delta 9/\Delta 9}$ adult zebrafish atrial cardiomyocytes have altered electrophysiology, related to Figure 5.

Quantification of action potential amplitude (APA, **A**), rest membrane potential (RMP, **B**), and upstroke velocity (**C**) of isolated *ttna*$^{+/+}$ (n = 5) and *ttna*$^{\Delta 9/\Delta 9}$ (n = 6) zebrafish atrial cardiomyocytes at 12 months old. Data are represented as mean ± 95% confidence intervals. ns $p > 0.05$; ** $p < 0.01$; **** $p < 0.0001$.

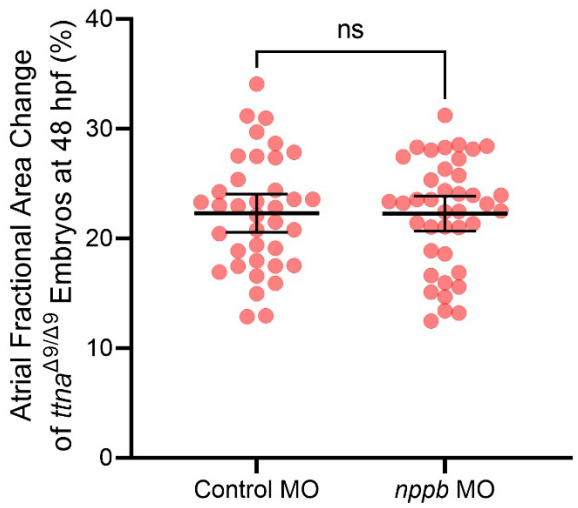

Figure S9. BNP knockdown cannot improve atrial contraction in *ttna*$^{\Delta 9/\Delta 9}$ zebrafish embryos, related to Figure 6.

Quantification for atrial contraction of Control MO-treated (n = 37) or *nppa* MO-treated (n = 40) *ttna*$^{\Delta 9/\Delta 9}$ zebrafish embryos at 48 hpf. Data are represented as mean ± 95% confidence intervals. ns $p > 0.05$.

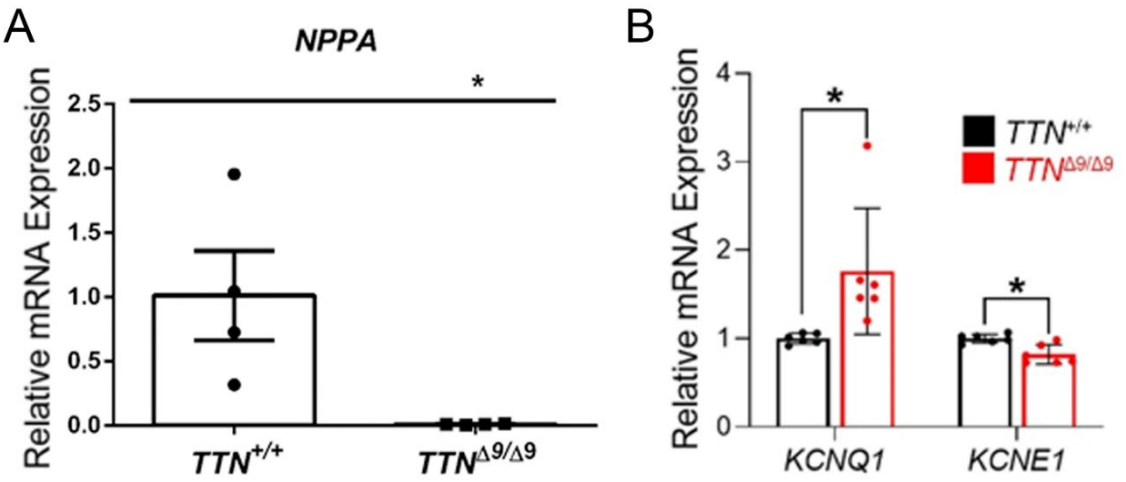

Figure S10. *TTN*$^{\Delta 9/\Delta 9}$-hiPSC-aCMs exhibit increased expression of *KCNQ1* and decreased expression of *NPPA* and *KCNE1*, related to Figure 6.
(**A**) Quantified relative *NPPA* gene expression in *TTN*$^{+/+}$-hiPSC-aCMs *and TTN*$^{\Delta 9/\Delta 9}$-hiPSC-aCMs (n=4 independent batches). (**B**) Quantified relative *KCNQ1* and *KCNE1* gene expression in *TTN*$^{+/+}$-hiPSC-aCMs *and TTN*$^{\Delta 9/\Delta 9}$-hiPSC-aCMs (n = 3 independent batches, n = 2 biological replicates per batch). Data are represented as mean ± 95% confidence intervals. * $p < 0.05$.

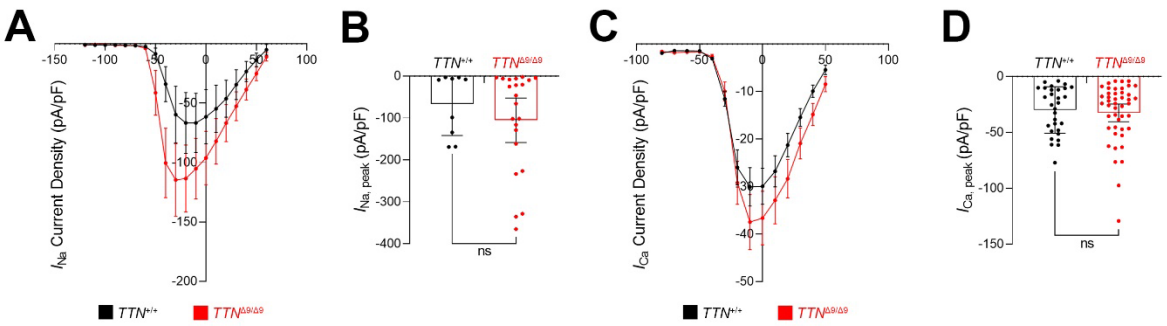

Figure S11. *TTN*$^{\Delta 9/\Delta 9}$-hiPSC-aCMs exhibit no significant difference in I_{Na} and I_{Ca} in comparison to *TTN*$^{+/+}$-hiPSC-aCMs, related to Figure 7.

Quantification of high-throughput voltage-clamp patch clamping targeting electrophysiology of I_{Na}, and I_{Ca} in *TTN*$^{+/+}$-hiPSC-aCMs and *TTN*$^{\Delta 9/\Delta 9}$-hiPSC-aCMs. (**A-B**) I_{Na} current-voltage (I-V) curves and quantification of I_{Na} densities at -10 mV (n = 12 for *TTN*$^{+/+}$; n = 37 for *TTN*$^{\Delta 9/\Delta 9}$). (**C-D**) I_{Ca} current-voltage (I-V) curves and quantification of I_{Na} densities at -10 mV (n = 30 for *TTN*$^{+/+}$; n = 46 for *TTN*$^{\Delta 9/\Delta 9}$). Data are represented as mean ± 95% confidence intervals. ns $p > 0.05$.

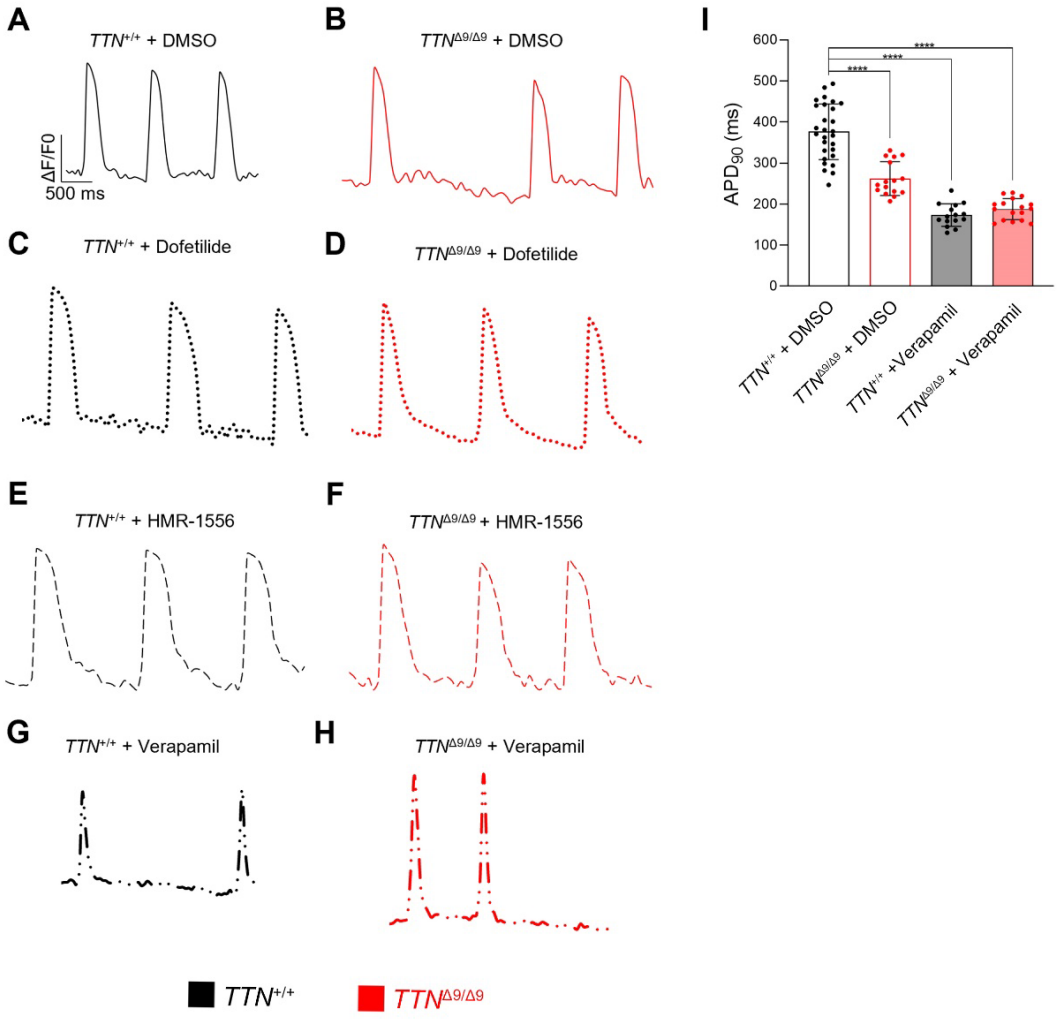

Figure S12. Ineffective recovery of electrophysiology phenotype in *TTN*$^{\Delta 9/\Delta 9}$-hiPSC-aCMs with calcium channel blockade, related to Figure 7.
(**A-H**) Representative tracing of action potential with optical voltage analysis on both *TTN*$^{+/+}$-hiPSC-aCMs and *TTN*$^{\Delta 9/\Delta 9}$-hiPSC-aCMs under treatment of DMSO (**A-B**), dofetilide (**C-D**), HMR-1556 (**E-F**) and verapamil (**G-H**). (**I**) Quantification of APD_{90} in hiPSC-aCMs under either DMSO or verapamil treatments. Data are represented as mean ± 95% confidence intervals. **** $p < 0.0001$.

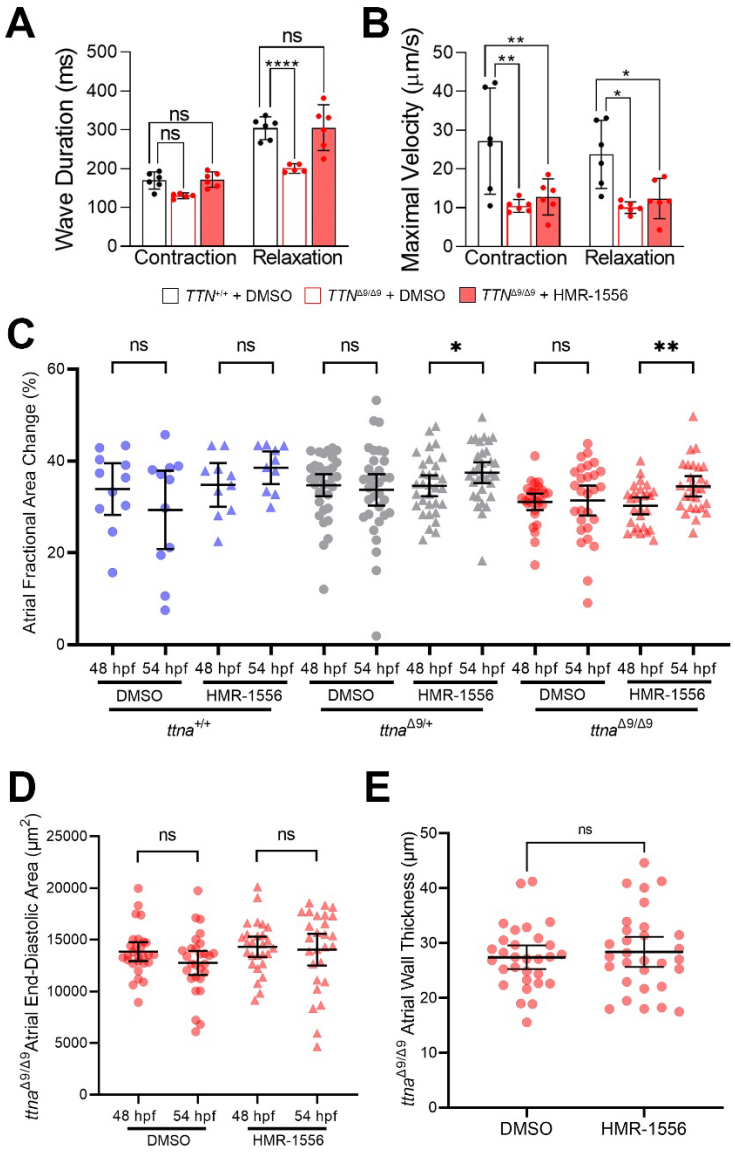

Figure S13. Blocking I_{Ks} rescues the contraction of *TTN*$^{\Delta 9/\Delta 9}$-hiPSC-aCMs and zebrafish atria, related to Figure 7.

(**A-B**) Quantification of wave component duration and maximal velocity of hiPSC-aCMs under the treatment of either DMSO or I_{Ks} blocker HMR-1556 in DMSO (2-way ANOVA with Bonferroni's correction) (n = 3 independent batches, n = 2 biological replicates per batch). (**C**) Quantification of zebrafish embryo atrial contraction under 10 μM HMR-1556/DMSO treatment from 50-54 hpf. n value: *ttna*$^{+/+}$-DMSO = 11; *ttna*$^{+/+}$-HMR-1556 = 10; *ttna*$^{\Delta 9/+}$-DMSO = 33; *ttna*$^{\Delta 9/+}$-HMR-1556 = 33; *ttna*$^{\Delta 9/\Delta 9}$-DMSO = 28; *ttna*$^{\Delta 9/\Delta 9}$-HMR-1556 = 27. *ttna*$^{\Delta 9/\Delta 9}$ columns are duplicated from Figure 7K. (**D**) Quantification of *ttna*$^{\Delta 9/\Delta 9}$ zebrafish embryo atrial end-diastolic area before and after 10 μM HMR-1556/DMSO treatment at 50-54 hpf. n value: DMSO-treated = 28; HMR-1556-treated = 27. (**E**) Quantification of *ttna*$^{\Delta 9/\Delta 9}$ zebrafish embryo atrial wall thickness at 96 hpf after 10 μM HMR-1556/DMSO treatment at 50-54 hpf. n value: DMSO-treated = 30; HMR-1556-treated = 30. Data are represented as mean ± 95% confidence intervals. ns $p > 0.05$; * $p < 0.05$; ** $p < 0.01$.

Table S1. Echocardiographic comparison of heart rate, ventricular size, and ventricular inflow velocities sorted by *ttna*$^{\Delta 9}$ genotype, related to Figure 4.

		Total Cohort		Wild-Type		Heterozygote		Mutant Homozygote		ANOVA	T-test*
		n	Mean (95% CI)	n	Mean (95% CI)	n	Mean (95% CI)	n	Mean (95% CI)	p-value	p-value
Heart Rate	BPM	34	102 (93, 112)	17	106 (90, 119)	10	104 (90, 119)	7	91 (72, 111)	0.4539	0.2641
Ventricular Volume	uL	28	1.16 (0.98, 1.33)	15	1.26 (1.01, 1.51)	6	1.14 (0.66, 1.62)	7	0.95 (0.53, 1.37)	0.3286	0.1435
Ventricular Area	mm2	32	1.28 (1.14, 1.41)	16	1.4 (1.22, 1.57)	9	1.14 (0.81, 1.48)	7	1.18 (0.83, 1.52)	0.2144	0.1793
Peak E Wave Velocity	mm/s	29	28.6 (23.0, 34.3)	12	30.6 (21.8, 39.3)	10	25.0 (15.2, 34.7)	7	30.6 (12.6, 48.5)	0.6449	0.9959
Peak A Wave Velocity	mm/s	34	244 (226, 261)	17	267 (245, 288)	10	222 (191, 253)	7	220 (169, 271)	**0.0226**	**0.034**

CI: Confidence Interval; BPM: Beats Per Minute; *: Comparison of means between Wild-Type and Mutant Homozygote Zebrafish

Table S2. List of qPCR primers or probes used in this study, related to STAR Methods.

	Forward Primer	Reverse Primer
nppa	GATGTACAAGCGCACACGTT	TCTGATGCCTCTTCTGTTGC
nppb	TGTTTCGGGAGCAAACTGGA	GTTCTTCTTGGGACCTGAGCG
neurod1	ACCACGAAGGGCATGAAACT	GTCCACGTCTCGTTCGTCTT
kcnq1	TTCACAGGGCCATCTCAACCTCAT	TCAAGCGCTCTGAACTTGTCTGGA
kcne1	CGCTCAAAGAAGGTGGAGAA	AAGAGCAGAAGGGTTGCTGA
rpl13	TCTGGAGGACTGTAAGAGGTATGC	AGACGCACAATCTTGAGAGCAG
NPPA	CAACGCAGACCTGATGGATTT	AGCCCCCGCTTCTTCATTC
KCNQ1	TaqMan probe: Hs00923522_m1 (ThermoFisher)	
KCNE1	TaqMan probe: Hs00899753_m1 (ThermoFisher)	
GAPDH	Taqman probe: Cat# 402869 (ThermoFisher)	